Published in final edited form as:

Otolaryngol Head Neck Surg. 2014 November ; 151(5): 751–759. doi:10.1177/0194599814547497.

Predicting post-surgery nasal physiology with computational modeling: current challenges and limitations

Dennis O. Frank-Ito, PhD[1], **Julia S. Kimbell, PhD**[2], **Purushottam Laud, PhD**[3], **Guilherme J. M. Garcia, PhD**[4,5], and **John S. Rhee, MD, MPH**[5]

[1]Division of Otolaryngology-Head and Neck Surgery, Duke University Medical Center, Durham, North Carolina

[2]Department of Otolaryngology/Head and Neck Surgery, University of North Carolina, Chapel Hill, North Carolina

[3]Division of Biostatistics, Institute for Health and Society, Medical College of Wisconsin, Milwaukee, Wisconsin

[4]Biotechnology & Bioengineering Center, Medical College of Wisconsin, Milwaukee, Wisconsin

[5]Department of Otolaryngology and Communication Sciences, Medical College of Wisconsin, Milwaukee, Wisconsin

Abstract

Introduction—High failure rates for surgical treatment of nasal airway obstruction (NAO) indicate that better diagnostic tools are needed to improve surgical planning. This study evaluates whether computer models based on a surgeon's edits of pre-surgery scans can accurately predict results from computer models based on post-operative scans of the same patient using computational fluid dynamics.

Study Design—Prospective study.

Setting—Academic medical center.

Methods—Three-dimensional nasal models were reconstructed from computed tomographic scans of 10 NAO patients pre- and 5–8 months post-surgery. To create transcribed-surgery models, the surgeon digitally modified the pre-operative reconstruction in each patient to represent physical changes expected from surgery and healing. Steady-state, laminar, inspiratory airflow was simulated in each model under physiologic, pressure-driven conditions.

Results—Transcribed- and post-surgery model variables were statistically different from pre-surgery variables at alpha=0.05. Unilateral nasal resistance and airflow were not statistically different between transcribed- and post-surgery models, but bilateral resistance was significantly different. Cross-sectional average pressures in transcribed-surgery trended with post-surgery. Transcribed-surgery prediction errors of post-surgery bilateral resistance were within 10–20% and

Address correspondence to: Dennis Onyeka Frank-Ito, Ph.D., Division of Otolaryngology - Head and Neck Surgery, Duke University Medical Center, Box 3805, Durham, NC 27710, dennis.frank@duke.edu, Phone: (919) 681-7247, Fax: (919) 613-6524.

There is no conflict of interest by any of the authors.

20–30% in 5 and 4 subjects, respectively. Prediction errors for unilateral resistance were <10%, 10–20% and 20–30% in 1, 2 and 4 subjects, respectively.

Conclusions—Computational models with modifications mimicking actual surgery and healing have the potential to predict post-operative outcomes. However, software to effectively translate virtual surgery steps into computational models is lacking. The ability to account for healing factors and the current limited virtual surgery tools are challenges that need to be overcome for greater accuracy.

Keywords

Nasal airway obstruction; Virtual surgery; Transcribed surgery; Computational fluid dynamics; Predominately obstructed side; Predicting post-surgery nasal physiology

Introduction

Nasal airway obstruction (NAO) is a common health condition that crosses many specialties of medicine, affects all age groups, and reduces overall quality of life.[1,2] The etiology of NAO consists of inflammatory conditions and anatomic deformities, such as septal deviation, hypertrophic turbinate, and incompetence of the nasal valve.[3,4] Surgery is predominately the treatment of choice for anatomic deformities, with septoplasty and/or turbinate surgery comprising more than half of the sinonasal procedures performed in the U.S. in 2006.[5]

The reported failure rate of surgical correction of nasal anatomic deformities is as high as 25–50%.[6–9] In addition, while short-term studies revealed patients' satisfaction rates ranging from 63–88%,[4,8,10] these rates waned over time.[11,12] Ho et al. [11] reported a steady decline in the number of patients who feel less obstructed over a period of 2.5 years post-operatively. Similarly, Jessen et al. [12] found that close to half of their patients reported NAO symptoms nine months post-surgery, and only about a quarter were symptom-free after 9 years. These failure rates could potentially be reduced if better diagnostic tools were available to guide surgical decision-making involving patient selection and most effective surgical techniques for each patient.

Ideally, the decision to perform surgery should not be based on clinical examination alone since NAO has multiple causes and often clinical examination cannot pinpoint cause for a given patient.[2] Current objective measures such as acoustic rhinometry and rhinomanometry for evaluation of nasal function have been found to correlate poorly with patients symptoms.[2,8,11,13] Advances in bioengineering computational techniques have the potential to fill this gap by providing consistent objective measures of nasal airflow and function.

The complex nature of the nasal airway motivates the creation of a computational tool to aid clinicians in the diagnosis and treatment of NAO. Anatomically accurate three-dimensional (3D) nasal geometries can be reconstructed from patient-specific computed tomographic (CT) or magnetic resonance imaging (MRI) scans. Computational fluid dynamics (CFD) techniques can be used to simulate airflow, heat transfer, and air humidification in the 3D nasal model. Furthermore, the nasal geometry can be virtually modified in a manner that

reflects surgical changes and new CFD simulations can be conducted to measure changes in nasal resistance, airflow allocation, and other variables of interest.[14] However, it is not known if 3D geometries reconstructed from hand-edited pixel selections on two-dimensional (2D) CT or MRI images can accurately mirror post-surgical changes.

This paper investigates the feasibility of surgeons' use of existing 2D editing tools in medical imaging software to create computational models that are predictive of nasal anatomy and physiology after post-surgical healing.

Materials and Methods

Patients and Treatment

Patients were recruited from the Medical College of Wisconsin (MCW) Otolaryngology clinic. Subjects were at least 15 years old, had a clinical diagnosis of non-reversible, surgically treatable cause for nasal obstruction (deviated septum, turbinate hypertrophy resistant to medical treatment, or lateral nasal wall collapse), elected to have nasal surgery, and provided written informed consent. Exclusion criteria included chronic sinusitis, nasal polyposis, and other forms of sinonasal disease. All the patients were otherwise healthy. The research described here was approved by the Institutional Review Board (IRB) at MCW. Diagnosis of NAO and surgical treatment decisions were made by the surgeon (J.S.R) based on clinical presentation and the standard of medical care.

Patients underwent one or more of the following standard surgical procedures: septoplasty, turbinectomy, septorhinoplasty and nasal valve repair (also known as vestibular stenosis repair) (Table 1). These procedures are the usual standard of care for treatment of NAO and are designed to improve airflow at the region of the nasal valve, as well as posteriorly. Rhinoplasty maneuvers and techniques included: tip rotation and refinement, lateral osteotomies, and dorsal reduction or augmentation. Unless specified otherwise, the rhinoplasty maneuvers were designed to change the external shape of the nose and overall were likely to contribute little to the nasal airflow parameters. Nasal valve repair maneuvers are listed in Table 1 and specified. The standard turbinectomy technique included cold steel debulking of the anterior two-thirds of the turbinate via bone resection and removal of the lateral mucosa and submucosa while preserving the medial mucosa. The remaining stump of the posterior one-third of the turbinate was then outfractured and lateralized. Post-surgical care was performed in the usual manner following nasal surgery with an uneventful post-operative course.

Pre- and post-surgical CT scans were obtained in all 24 patients enrolled in this study at the time of this report; these scans were performed on study participants and are not routinely indicated in the surgeon's practice. Four patients were excluded from the analysis presented here due to having functional endoscopic surgery before or in addition to treatment for NAO, and one subject was excluded due to an unrepaired anatomical defect in the nasal vestibule; thus high-resolution CT scans for 19 patients were available for analysis. To prevent any confounding effects of nasal cycling on modeling results, the 10 patients in whom mucosal thickness was generally symmetrical in both pre- and post-operative CT

were selected for this analysis. To allow for adequate healing, post-operative CT scans were performed 5– 8 months after surgery.

Nasal Model Reconstruction

Pre- and post-operative CT scans were imported into a medical imaging software package (Mimics™ 13.1, Materialise, Inc., Plymouth, MI) and 3D reconstructions of each patient's nasal airspaces, excluding the paranasal sinuses, were created. To construct the transcribed-surgery models, the surgeon (J.S.R) reproduced the surgery performed on each patient by hand-editing the pre-surgery Mimics™ file as soon after the surgery as possible, and before studying postoperative scans and reconstructions. The 3D transcribed-surgery (TS) models were hypothesized to reflect anatomical changes expected to arise from the actual surgery (Figure 1). In accordance with the IRB protocol, transcribed-surgery models were created after actual surgery was performed so that surgical decision making would not be influenced by CFD results, since the ability of CFD to predict patient outcomes has not been demonstrated. The transcribed-, pre- and post-surgery nasal reconstructions were exported from Mimics™ and imported into the CAD and mesh-generating software package ICEM-CFD™ 12.1 (ANSYS, Canonsburg, PA) where planar nostril and outlet surfaces were constructed.

CFD Simulation

To solve the equations that govern fluid flow, unstructured tetrahedral meshes were generated in ICEM-CFD™ using approximately 4 million graded elements, indicated by an in-house mesh density study to provide mesh-independent numerical results. Mesh quality analysis ensured that all tetrahedral elements had an aspect ratio greater than 0.3 to prevent distorted elements from affecting the accuracy of the numerical simulation. Steady-state laminar inspiratory airflow was simulated using the CFD software package Fluent™ 12.1.4 (ANSYS, Inc., Canonsburg, PA) under physiologic pressure-driven conditions. Although nasal airflow may become turbulent at higher flow rates occurring during sniffing or exercise, there is evidence that laminar conditions dominate nasal airflows at resting to moderate breathing rates,[15,16] as in the present study.

The boundary conditions to determine airflow were: (1) "wall" condition assuming that the walls were stationary with zero velocity at the air-wall interface; (2) "pressure-inlet" condition at the nostrils with gauge pressure set to zero; (3) "pressure-outlet" condition at the outlet with gauge pressure set to a negative value that generated a target steady-state flow rate in the post-surgery model. This flow rate was twice the minute volume, which was estimated from body weight using gender-specific power law curves.[17] In the pre- and transcribed-surgery models, the boundary condition for pressure at the outlet was set to achieve similar pressure gradient from the nostrils to the posterior end of the nasal septum as in the post-surgery model.

Outcome Measures

The outcome measures computed for comparing CFD simulations in pre-, transcribed-and post-surgery models were nasal resistance (NR); unilateral airflow; and coronal cross-sectional average pressure. Bilateral and unilateral NR were calculated as $\Delta p/Q$, where Δp is

the trans-nasal static pressure drop from the nostril(s) to the posterior end of the septum and Q is the flow rate. Unilateral airflow on the predominately obstructed side (POS) was total flow passing through this side of the nasal cavity. Cross-sectional POS average pressure along varying distances from the tip of the nostril to the posterior end of the septum was compared in pre-, transcribed-, and post-surgery models for each individual.

Statistical Analysis

The two tailed non-parametric Wilcoxon Signed-Rank test for paired samples was used to test the null hypotheses that CFD-computed NR and POS airflow in:

1. Pre-surgery models were not statistically different from post-surgery models.
2. Transcribed-surgery models were not statistically different from pre-surgery models.
3. Transcribed-surgery models were not statistically different from post-surgery models.

A p-value < 0.05 was taken to imply statistical significance. Statistical analyses were performed using Microsoft Excel™ 2010 (Microsoft Corp., Redmond, WA, USA), the Excel add-in Real Statistics Resource Pack (www.real-statistics.com) was used in conducting the non-parametric Wilcoxon Signed-Rank test. Relative differences between patients' transcribed-surgery model predictions and their respective post-surgery model results (relative prediction error) were quantified for bilateral and POS NR, as well as POS airflow:

$$\text{Relative Prediction Error} = \frac{|TS - Post|}{Post}\%,$$

where *TS* is transcribed-surgery model prediction and *Post* is post-surgery model result.

Results

Pairwise difference comparing pre-, post-, and transcribed-surgery nasal models are provided in Table 2. Kimbell et al. [18] described differences between pre- and post-surgery nasal models in NR (bilateral p=0.038 and POS p=0.029) and in POS airflow (p<0.001), and showed that average bilateral and POS NR values in the pre-surgery models were higher than in post-surgery (Figure 2). Tests of hypotheses (Table 2) between pre- and transcribed-surgery models also showed significant differences in both bilateral (p=0.005) and POS (p=0.005) NR, as well as POS airflow (p=0.005). These results are consistent with our expectation since transcribed-surgery models were modified to mimic actual surgical changes; as post-surgery models were different from pre-surgery, we anticipate that transcribed-surgery models will be different from pre-surgery. Tests of hypotheses between transcribed- and post-surgery models (Table 1) indicated that both POS NR (p=0.059) and POS airflow (p=0.074) were not significantly different, but in contrast to our expectation, bilateral NR was significantly different (p=0.047). NR values were on average lower in the transcribed-surgery models than in post-surgery models, and corresponding transcribed-surgery POS airflow was on average higher than in post-surgery models (Fig. 2).

Another way we investigated the accuracy of the surgeon's transcribed-surgery models was to plot transcribed-surgery variables versus post-surgery variables (Figure 3). In these plots, the solid line corresponds to the case when transcribed-surgery variables are a perfect match to post-surgery results. These plots reveal that transcribed-surgery models captured post-surgery NR values better than POS airflow and that transcribed-surgery had a tendency to over-estimate the effect of surgery on POS airflow.

Transcribed-surgery relative prediction errors of post-surgery models are presented in Figure 4 for computed bilateral and POS NR, as well as POS airflow. For bilateral NR, the relative prediction errors were within 10–20% in 5 subjects, 20–30% in 4 subjects, and 30–40% in 1 subject. For POS NR, relative prediction errors were as follows: <10% in 1 subject, 2 subjects had errors within 10–20% and 30–40%, respectively; 3 subjects within 20–30% and >40% in 1 subject. Prediction errors for POS airflow had 2 subjects <10%, 20–30%, and 30–40%, respectively; 1 subject within 10–20% and 3 subjects were >40%.

The results for cross-sectional POS average pressure as a function of distance from the tip of the nostril to the choana are shown in Figure 5. Cross-sectional pressure in transcribed-surgery models consistently trended with post-surgery pressure in four subjects (1, 4, 6, and 10); upstream and downstream effects in post-surgery pressure beyond regions of surgical change were accurately captured by transcribed-surgery models. In addition, a relatively good agreement in cross-sectional pressure for five other subjects (2, 5, 7, 8, and 9) was also observed; while subject 3 had little or no agreement (Fig. 5a).

Discussion

Bailie et al. [19] postulated that one of the potential applications of computational modeling of nasal airflow is surgical planning aimed at relieving NAO. Several research groups are currently pursuing the long-term objective of developing surgery-planning methods using CFD to allow surgeons to design patient-specific surgical interventions that optimize surgical outcomes. In this context, the goal of this report was to investigate the potential for post-surgery nasal physiology, assessed by CFD, to be predicted by digital manipulation of 3D nasal models constructed from pre-operative nasal anatomy using current technology. Although many studies have used digitally-altered nasal models to investigate airflow in the nose,[2,10,14,20,21] the present study is the first, to our knowledge, to compare CFD variables predicted by digitally transcribed-surgery models to values obtained in models based on the actual post-surgery anatomy in more than one subject.

CFD techniques involving virtual surgery have previously been studied in a single NAO subject.[14,20] In an earlier study by our group, three virtual surgery models were created from a pre-operative CT scan (right inferior turbinate reduction (ITR), septoplasty, and septoplasty with right ITR) and compared with actual post-surgical outcomes.[14] In another study, Rhee and colleagues[20] used virtual surgery techniques to quantify effects of individual components of nasal airway surgery in a patient who underwent septoplasty, bilateral turbinate reduction, and nasal valve repair. Lastly, Ozlugedik and colleagues[2] performed virtual septoplasty and partial turbinectomy from a cadaveric scan to investigate effects of septal deviation and concha bullosa on nasal airflow. The current study extends

these efforts to a larger cohort for statistical analysis of the effects of digital manipulations of pre-surgery models to predict post-surgical outcomes.

To compare pre-, transcribed- and post-surgery models objectively, we studied CFD variables that are relevant to symptoms of nasal congestion, namely NR, airflow and pressure. Preliminary data from our 4-year study suggest that bilateral and POSNR, airflow, and heat fluxes are significantly different in pre- and post-surgical CFD models.[18] In addition, POS airflow ($r=-0.7$) and heat fluxes ($r=-0.65$) moderately correlated with patient's subjective feeling of obstruction, while NR had a weaker correlation ($r=0.48$).[18] Correlations of bilateral NR, airflow, and heat flux with patient-reported measures were 0.33, −0.54 and −0.45, respectively. Therefore, these variables are candidates to be used in predicting patient-reported outcomes from future virtual surgery tools that accurately describe expected changes from NAO surgery and healing.

By comparing pre-surgery versus post-surgery geometries, we established that pre-surgery nasal anatomy was significantly different from post-surgery anatomy in every CFD-derived variable computed, suggesting that surgery had a real impact in this cohort of patients. In addition, by showing that there is a significant change between pre-surgery geometries and transcribed-surgery models based on pre-operative CT scans, we demonstrated that modifications made on the transcribed-surgery models do indeed intend to reflect actual surgical results. Figure 5 demonstrates that virtual surgery generally mirrored actual surgery in terms of specific anatomical areas that were changed. However, it is apparent that transcribed-surgery had a tendency to over-predict reduction in NR and the increase in nasal airflow, indicating that the surgeon tended to over-estimate the benefit of surgery. For example, data points of 8 out of 10 subjects fell below the line for bilateral NR (Figure 3A).

There are also challenges with current editing tools available for medical images that limit the surgeon's ability to accurately transcribe how each procedure was done in the operating room on the computer. With regard to translation of actual surgical steps into the transcribed-surgery models, as previously indicated, the software used (Mimics™ 13.1) required manual editing of 2-dimensional cross-sections. This method was crude, labor-intensive, and possibly prone to errors because the surgeon did not have access to familiar, 3-dimensional views as would be experienced during actual surgery. Another potential source of variability between transcribed- and post-surgery models was the assumption that the engorgement state of the nasal mucosa was similar before and after surgery. Given these sources of error, we did not expect 100% accuracy between transcribed-surgery and post-surgery models. In fact, we interpret our results as evidence that transcribed-surgery modeling will in the near future predict post-surgery nasal physiology, as measured by CFD. Our results also suggest that editing 2-dimensional cross-sections is not the most effective way of performing transcribed-surgery. Future studies should develop methods to alter the nasal geometry in three dimensions and provide surgeons an endoscopic view that is closer to their experience in the operating room.

The results presented here indicate that computational methods show significant promise as a potential useful tool in preoperative nasal surgical planning, but current editing tools for 3D segmentations are "not ready for prime time". Continuous advancement in current

medical image analysis software is required before computational tools that can be used by surgeons for accurate diagnosis and surgical planning of NAO can be developed. An additional limitation of the current study is a reliance on assumptions that (1) images at a specific time point adequately represented the nasal anatomy despite the dynamic nature of the nasal mucosa, (2) breathing occurred via the nose alone when in reality patients with NAO can also breathe through the mouth, (3) steady-state simulation captured the main features of rhythmic breathing, and (4) inter-individual variability in post-surgical healing was insignificant. Further study is needed to assess the potential effects of these assumptions on conclusions using CFD variables. Nonetheless, with the rapid rate of technological advances, it is not difficult to envision a future where nasal surgeons will be able to use validated CFD-aided virtual surgery tools with imaging data in an environment that can perform quick and precise in-office analyses to identify problematic regions, as well as simulate the effects of surgical interventions within minutes.

In conclusion, this study shows that digitally modified computational models based on pre-operative CT scans reflecting actual surgical interventions can potentially predict post-surgery nasal physiology, with variability due to translation of actual surgical steps to the computer model and imprecise modeling of the effects of post-surgical healing or actual intraoperative interventions. The findings in this study lay the groundwork for the development of future pre-surgical predictive modeling and virtual surgery tools with the ultimate goal of improved outcomes for patients with NAO.

Acknowledgments

This research was funded by grants R01EB009557 and R01EB009557-01S1 from the National Institutes of Health/ National Institute of Biomedical Imaging and Bioengineering under subcontract to the University of North Carolina from the Medical College of Wisconsin. This manuscript is solely the responsibility of the authors and does not represent the official views of the NIH. The authors thank Nicole Stelse for her contributions to this work.

References

1. Rhee JS, Book DT, Burzynski M, Smith TL. Quality of life assessment in nasal airway obstruction. Laryngoscope. 2003; 113:1118–1122. [PubMed: 12838007]
2. Ozlugedik S, Nakiboglu G, Sert C, et al. Numerical study of the aerodynamic effects of septoplasty and partial lateral turbinectomy. Laryngoscope. 2008; 118:330–334. [PubMed: 18030167]
3. Rhee JS, Poetker DM, Smith TL, Bustillo A, Burzynski M, Davis RE. Nasal valve surgery improves disease-specific quality of life. Laryngoscope. 2005; 115:437–440. [PubMed: 15744153]
4. Roblin DG, Eccles R. What, if any, is the value of septal surgery? Clin Otolaryngol Allied Sci. 2002; 27:77–80. [PubMed: 11994109]
5. Bhattacharyya N. Ambulatory sinus and nasal surgery in the United States: demographics and perioperative outcomes. Laryngoscope. 2010; 120:635–638. [PubMed: 20058315]
6. Singh A, Patel N, Kenyon G, Donaldson G. Is there objective evidence that septal surgery improves nasal airflow? J Laryngol Otol. 2006; 120:916–920. [PubMed: 17040608]
7. Andre RF, D'Souza AR, Kunst HP, Vuyk HD. Sub-alar batten grafts as treatment for nasal valve incompetence; description of technique and functional evaluation. Rhinology. 2006; 44:118–122. [PubMed: 16792170]
8. Dinis PB, Haider H. Septoplasty: long-term evaluation of results. Am J Otolaryngol. 2002; 23:85–90. [PubMed: 11893975]

9. Illum P. Septoplasty and compensatory inferior turbinate hypertrophy: long-term results after randomized turbinoplasty. Eur Arch Otorhinolaryngol. 1997; 254 (Suppl 1):S89–92. [PubMed: 9065637]
10. Garcia GJ, Rhee JS, Senior BA, Kimbell JS. Septal deviation and nasal resistance: an investigation using virtual surgery and computational fluid dynamics. Am J Rhinol Allergy. 2010; 24:e46–53. [PubMed: 20109325]
11. Ho WK, Yuen AP, Tang KC, Wei WI, Lam PK. Time course in the relief of nasal blockage after septal and turbinate surgery: a prospective study. Arch Otolaryngol Head Neck Surg. 2004; 130:324–328. [PubMed: 15023841]
12. Jessen M, Ivarsson A, Malm L. Nasal airway resistance and symptoms after functional septoplasty: comparison of findings at 9 months and 9 years. Clin Otolaryngol Allied Sci. 1989; 14:231–234. [PubMed: 2743612]
13. Pawar SS, Garcia GJ, Kimbell JS, Rhee JS. Objective measures in aesthetic and functional nasal surgery: perspectives on nasal form and function. Facial Plast Surg. 2010; 26:320–327. [PubMed: 20665410]
14. Rhee JS, Pawar SS, Garcia GJ, Kimbell JS. Toward personalized nasal surgery using computational fluid dynamics. Arch Facial Plast Surg. 2011; 13:305–310. [PubMed: 21502467]
15. Shanley KT, Zamankhan P, Ahmadi G, Hopke PK, Cheng YS. Numerical simulations investigating the regional and overall deposition efficiency of the human nasal cavity. Inhal Toxicol. 2008; 20:1093–1100. [PubMed: 18800272]
16. Kelly JT, Prasad AK, Wexler AS. Detailed flow patterns in the nasal cavity. J Appl Physiol. 2000; 89:323–337. [PubMed: 10904068]
17. Garcia GJ, Schroeter JD, Segal RA, Stanek J, Foureman GL, Kimbell JS. Dosimetry of nasal uptake of water-soluble and reactive gases: a first study of interhuman variability. Inhal Toxicol. 2009; 21:607–618. [PubMed: 19459775]
18. Kimbell JS, Frank DO, Laud P, Garcia GJ, Rhee JS. Changes in nasal airflow and heat transfer correlate with symptom improvement after surgery for nasal obstruction. J Biomech. 2013; 46:2634–2643. [PubMed: 24063885]
19. Bailie N, Hanna B, Watterson J, Gallagher G. An overview of numerical modelling of nasal airflow. Rhinology. 2006; 44:53–57. [PubMed: 16550951]
20. Rhee JS, Cannon DE, Frank DO, Kimbell JS. Role of Virtual Surgery in Preoperative Planning: Assessing the Individual Components of Functional Nasal Airway Surgery. Arch Facial Plast Surg. 2012
21. Grant O, Bailie N, Watterson J, Cole J, Gallagher G, Hanna B. Numerical model of a nasal septal perforation. Stud Health Technol Inform. 2004; 107:1352–1356. [PubMed: 15361035]

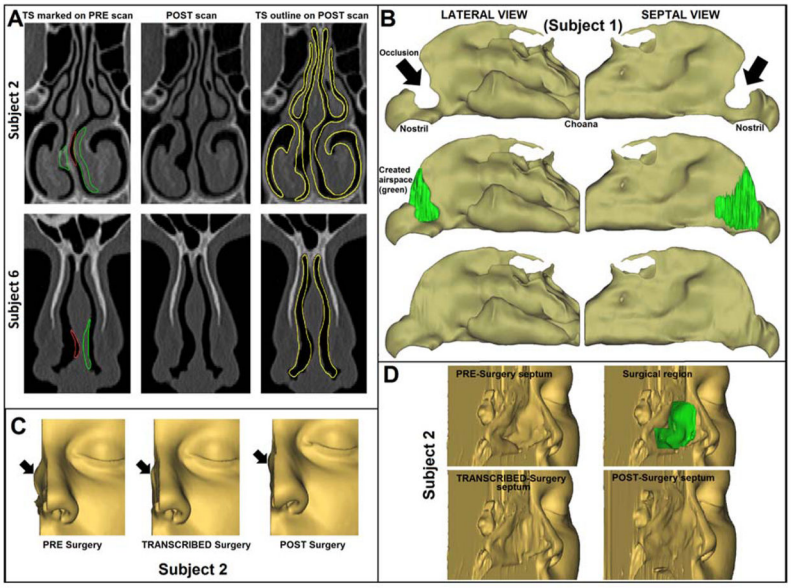

Figure 1.

(A) (LEFT) digitally created airspace (green), and closed airspace (red). (RIGHT) Transcribed-surgery (yellow) superimposed on post-surgery. (B) (TOP) pre-surgery airspace; (MIDDLE) Surgeon's edits on pre-surgery; (BOTTOM) Transcribed-surgery airspace after smoothing. (C) Septal deviation. (D) Nasal septum.

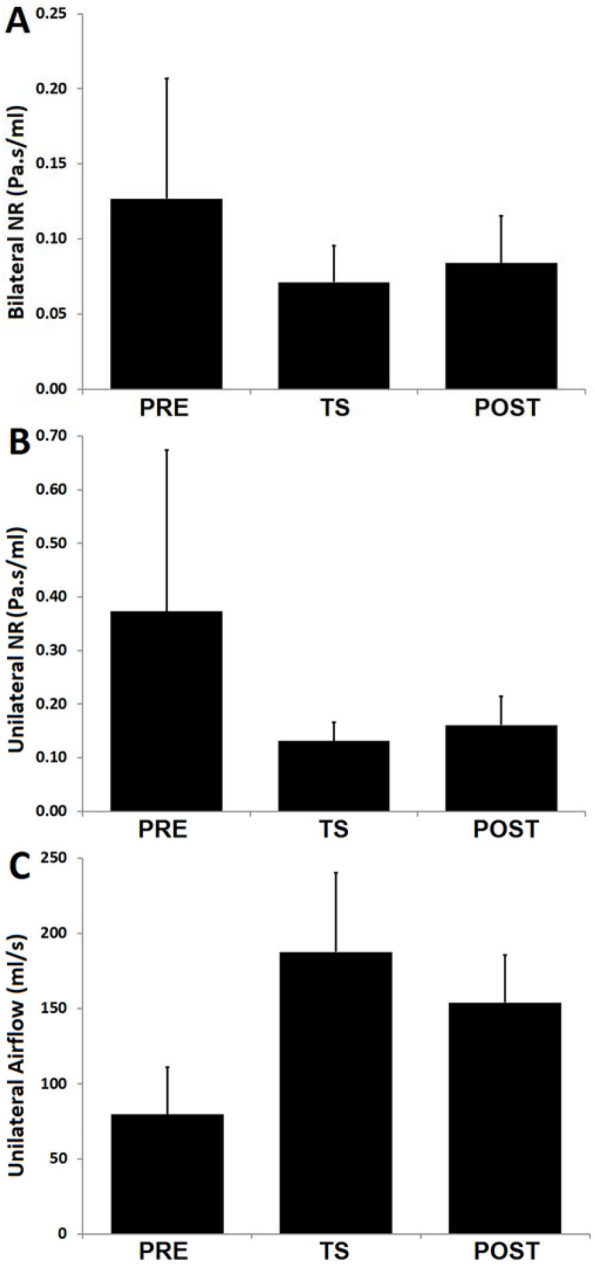

Figure 2.

Average (n=10) CFD-derived variables comparing pre-surgery (PRE), transcribed-surgery (TS), and post-surgery (POST). (A) Bilateral NR. (B) Predominately obstructed side NR. (C) Predominately obstructed side airflow. Error bars correspond to one standard deviation. NR= Nasal resistance.

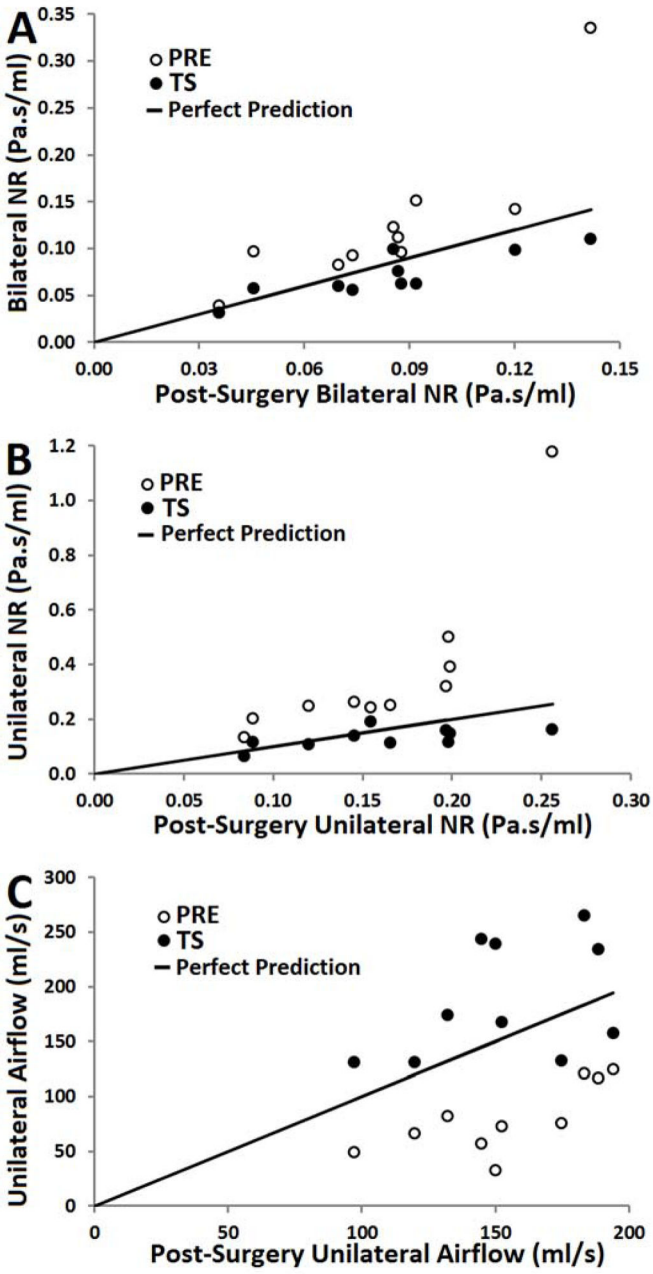

Figure 3.

Transcribed-surgery versus post-surgery and pre-surgery versus post-surgery. Solid line indicates transcribed-surgery ideal prediction. (A) Bilateral NR. (B) NR on the predominately obstructed side. (C) Airflow on the predominately obstructed side. NR=Nasal resistance; PRE=Pre-surgery; TS=Transcribed-surgery.

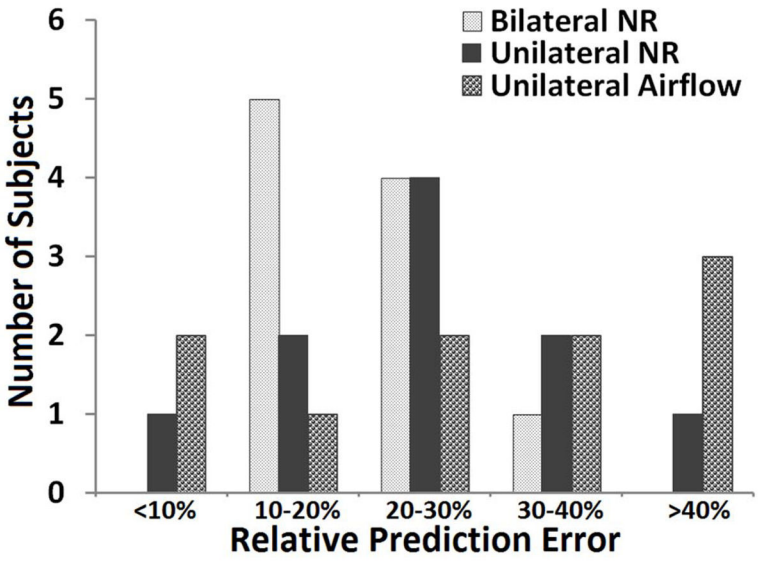

Figure 4.

Relative error of transcribed-surgery prediction of post-surgery for CFD computed variables (n=10). Each bar indicates the number of subjects with relative prediction errors within a given percentage range. NR = Nasal resistance.

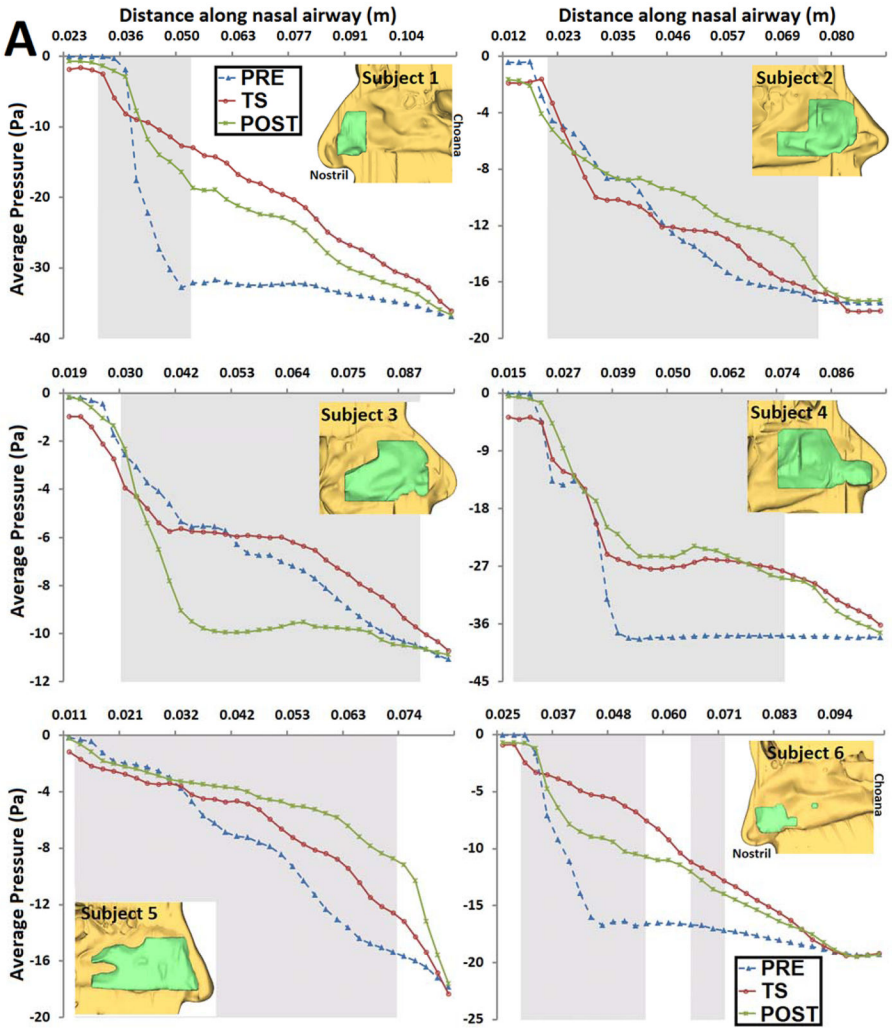

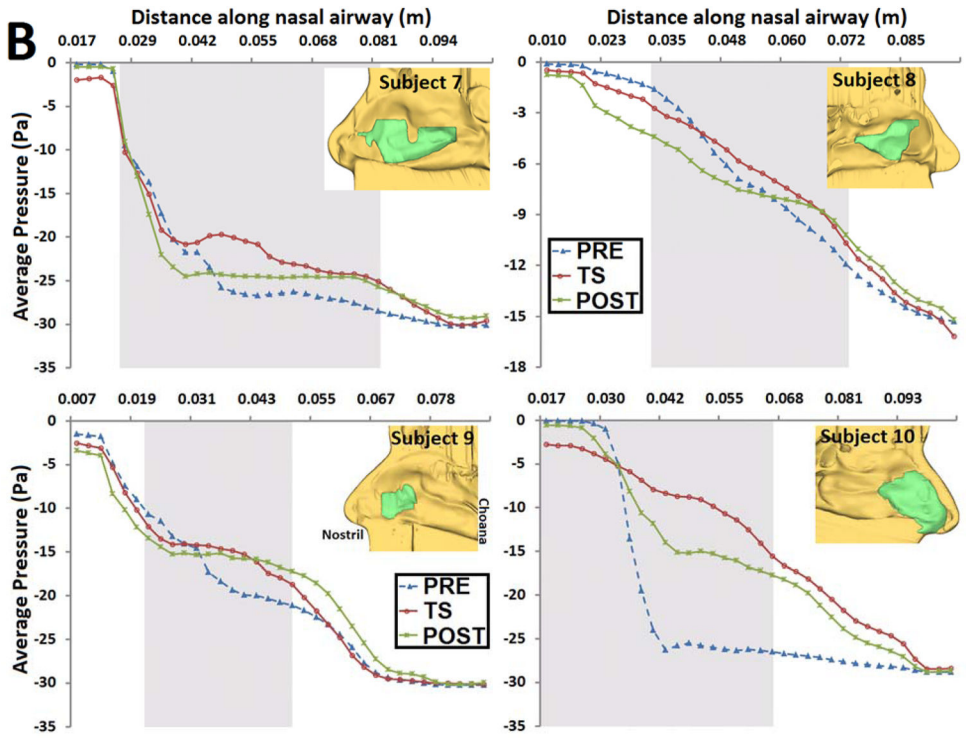

Figure 5.

Average pressure comparisons at varying distance along the nasal passage on the predominately most obstructed side. Grey vertical bar shows surgical region, which corresponds to green region on the septum. PRE=Pre-surgery; TS=Transcribed-surgery; POST=Post-surgery.

Table 1

Diagnoses and surgical procedures in a cohort of 10 individuals with nasal obstruction.[18]

Subject (Gender)	Age	Diagnoses	Predominant side of obstruction	Surgical procedure
1 (male)	38	Deviated nasal septum External nasal deformity	Left	Septorhinoplasty
2 (female)	27	Deviated nasal septum External nasal deformity Inferior turbinate hypertrophy	Right	Septorhinoplasty Turbinectomy
3 (male)	38	Deviated nasal septum External nasal deformity	Right	Septorhinoplasty
4 (male)	33	Deviated nasal septum External nasal deformity Inferior turbinate hypertrophy	Right	Septorhinoplasty Turbinectomy
5 (female)	53	Deviated nasal septum Bilateral vestibular stenosis Bilateral inferior turbinate hypertrophy	Right	Septoplasty Repair of bilateral vestibular stenosis with butterfly onlay graft Bilateral turbinectomy
6 (female)	22	Deviated nasal septum Bilateral vestibular stenosis	Left	Septoplasty Repair of bilateral vestibular stenosis
7 (male)	38	Deviated nasal septum Inferior turbinate hypertrophy	Left	Septoplasty Turbinectomy
8 (male)	46	Deviated nasal septum External nasal deformity Inferior turbinate hypertrophy	Right	Septorhinoplasty Turbinectomy
9 (male)	34	Deviated nasal septum Bilateral inferior turbinate hypertrophy	Left	Septoplasty Bilateral turbinectomy
10 (male)	45	Deviated nasal septum External nasal deformity Bilateral vestibular stenosis	Right	Septorhinoplasty Repair of bilateral vestibular stenosis with spreader grafts

Table 2

Pairwise differences comparing pre-surgery (PRE), post-surgery (POST), and transcribed-surgery (TS) for CFD-derived bilateral and predominately obstructed side variables. A p-value<0.05 implies statistically significant differences between model types.

CFD-Derived Variable	Pairwise Difference	Mean	Standard Deviation	P-Value (Non-parametric)
Bilateral NR (Pa.s/ml)				
	PRE & POST	0.043	0.056	0.005
	PRE & TS	0.056	0.063	0.005
	POST & TS	0.013	0.016	0.047
Unilateral NR (Pa.s/ml)				
	PRE & POST	0.212	0.259	0.005
	PRE & TS	0.242	0.289	0.005
	POST & TS	0.030	0.043	0.059
Unilateral Flow (ml/s)				
	PRE & POST	73.975	22.560	0.005
	PRE & TS	107.755	56.323	0.005
	POST & TS	33.779	48.763	0.074